Indian Journal of Science and Technology, *Vol 9(7), DOI: 10.17485/ijst/2016/v9i7/78751, February 2016*
ISSN (Print) : 0974-6846
ISSN (Online) : 0974-5645

Comparative Analysis of Two Level VSI and Three Level Neutral Point Clamped Inverter for Torque Ripple Reduction in Induction Drive

P. Rajasekaran[1*] and V. Jawahar Senthilkumar[2]

[1]Department of Electrical and Electronics Engineering, Jawaharlal Nehru Technological University, Hyderabad - 500085, Telangana, India; rajasekaranphd123@gmail.com
[2]Department of Electronics and Communication Engineering, Anna University, Chennai –600025, Tamil Nadu, India; veerajawahar@yahoo.com

Abstract

This paper presents the comparative analysis of various level of multilevel inverter for induction motor torque ripple minimization. The neutralpoint clamped (NPC) inverter is used an adequate solution in AC drives application. The Conventional inverters compared to multilevel inverters have many limitations in high-voltage and high-power applications like poor power quality, high voltage stress, EMI/EMC issue etc. Also proposed the Space Vector neutral point clamped inverter for Torque ripple reduction in induction drive. The Simple Space vector control scheme is applied to neutral point clamped inverter by reference torque estimation. In this proposed topology offer an improved performance in the form of torque ripple reduction scheme. The Classical direct torque control of two-level VSI scheme is compared with proposed three-level NPC scheme. The main aim of this paper to provide a significant method and control scheme to obtained torque ripple reduction in induction motor Drive. The result shows the performance of neutral point clamped inverter using CB-PWM on induction drive. In this paper three levels VSI based Neutral Point Clamped (NPC) multilevel inverter fed induction motor drive is simulated, analyzed and compared with two levels VSI based NPC inverter drives. Torque of the motor is controlled by using space vector based direct torque control (DTC) method. The simulation results are carried out by using MATLAB/SIMULAINK environment.

Keywords: Direct Torque Control (DTC), Induction Drive, Multilevel Inverter, Neutral Point Clamped Inverter (NPC), Space Vector Pulse Width Modulation (SVPWM), Torque Ripple, Voltage Source Inverter (VSI)

1. Introduction

Recently, the growth of high power, low cost and authentic power electronic converters causes an opportunity of using medium or large induction machines in advanced industrial drive applications[1]. The Direct torque control is a powerful control scheme for induction motor torque ripple control. The conventional hysteresis based DTC algorithm for voltage switching method has relative merits of simple structure and easy implementation[2].

Currently various decades of investigation, many DTC strategies have been proposed so far. The four major categories such as band-constrained technique[3], Space Vector Modulation (SVM)-based control of the switching frequency[4,5] and strategies using predictive control schemes[6] and finally the hybrid PWM (Pulse Width Modulation) technique[7]. The Power Factor Correction (PFC) based control strategies used for torque ripple of BLDC Drive[8]. Nonetheless, the improved performance is federal to significant growth of implementation schemes.A direct torque control of two-level inverter for switching frequencies control ranges 2–3 kHz, theSwitching frequency is operated below 1 kHzcauses some limitation in torque ripple reduction[9].Two-level Inverter switching frequency is restricted in variable switching frequency andit is not applicable in high power drive applications[10].

**Author for correspondence*

Present work deal with comparison in performance of Torque ripple reduction fed induction motor drive using two levels VSI and three-level neutral point clamped inverter schemes[11]. The basic problemsare associated with the conventional DTC control methods because of high torque ripple, variable switching frequency and performance deterioration at low, near to zero speed basic. Limitation of classical controller has two to three control loops are presented for torque and flux control[12,14].

The standard multilevel inverter topology discussed with two-level inverter topology, multilevel inverter is a most prominent solution for induction motor drive. The Multilevel must be used to reduce the harmonics and high switching frequency with low switching losses. Three-level inverter is popularly used in high power drives application[15,16]. A lot of research have been done in neutral point clamped multilevel inverter topology and a numerous of control methods have been presented in the literature stand on ripple minimization in induction motor[17,18]. An active Neutral Point Clamped inverter (NPC) fed BLDC drive used to analysis the minimization of torque ripple and reduction of harmonics[19].

The modeling of induction machine[20, 21] is referred by using the reference frame of theory. The total harmonic distortion of neutral point diode clamped inverter is analyzed for solar power applications. The comparative analysis of multilevel inverter is carried out under various PWM techniques[22, 23]. The optimized harmonic elimination is analyzed by phase disposition and phase shifting PWM method[24].

In this paper analyzed the suitable topology for torque ripple minimization by comparing the direct torque control of two level VSI(Voltage Source Inverter) and three level NPC-VSI(neutral point clamped- voltage source inverter). In principle, DTC method based on simple space vector modulation scheme is introduced for torque ripple reduction. Additional factors of proposed control scheme are DC-Link balancing control, current ripple reduction and flux control. A simple space vector scheme is changes in same direction with respect to level of positive and negative variation over DTC two-level scheme. The rest of the paper is organized as follows: sections II described about the induction machine and DTC with two-level VSI. Sections III described about DTC with the three-level NPC-VSI topology. The DTC based SVM strategy is discussed at section IV so the comparison simulation results are exposed at the next section. Finally, conclusions are given in the last section.

2. Theory

2.1 Modeling of Machine

An induction Machine is modeled using voltage and flux equations which are referred to a general reference frame, denoted by the superscript "g" and are shown as follows[17,18].

Stator voltage equation:

$$v_s^g = i_s^g r_s + jw_g \lambda_s^g + p\lambda_s^g . \tag{1}$$

Rotor voltage equation:

$$0 = i_r^g R_r + j(w_g - w_r)\lambda_r^g + p\lambda_r^g . \tag{2}$$

Stator flux equation:

$$\lambda_s^g = L_s i_s^g + L_m i_r^g . \tag{3}$$

Rotor flux equation:

$$\lambda_r^g = L_r i_s^g + L_m i_r^g . \tag{4}$$

Mechanical equation:

$$T_e - T_L = j_m p w_r + B_m w_r \tag{5}$$

$$T_e = \frac{3P}{4}(\lambda_{ds}^g i_{qs}^g - \lambda_{qs}^g i_{ds}^g) \tag{6}$$

By referring to a stationary frame, denoted by the superscript "α," which is with d -axis attached on the stator winding of Phase " A," the mathematical equations of induction motor can be rewritten as follow

Stator voltage equation:

$$v_s^\alpha = i_s^\beta R_s + p\lambda_s^\alpha \tag{7}$$

Rotor voltage equation:

$$0 = i_r^\alpha R_r - jw_r \lambda_r^\alpha + p\lambda_r^\alpha \tag{8}$$

Stator flux equation:

$$\lambda_s^\alpha = L_s i_s^\alpha + L_m i_r^\alpha . \tag{9}$$

Rotor flux equation

$$\lambda_r^\alpha = L_r i_r^\alpha + L_m i_s^\alpha \tag{10}$$

Mechanical equation:

$$T_e - T_L = j_m p w_r + B_m w_r \tag{11}$$

$$T_e = \frac{3P}{4}(\lambda_{ds}^\alpha \lambda_{qs}^\alpha - \lambda_{qs}^\alpha \lambda_{ds}^\alpha) \tag{12}$$

Substituting (9) and (10) into 12, yields

$$T_e = \frac{3P}{4}\frac{L_m}{\sigma L_s L_r}(\lambda_{ds}^a \lambda_{qr}^a - \lambda_{qs}^a \lambda_{dr}^a) \tag{13}$$

Where σ = Total leakage factor, $\sigma \equiv 1 - L_m^2 / L_s L_r$

2.2 DTCBasis

DTC topologies allows a direct control of the motor variables through a suitable selection of the inverter control signals, the stator flux and torque are need to be increased, decreased, or maintained for fulfill the requirement of drive. These decisions are made by output $c\varphi$ of the flux dynamic of Φs is governed by the stator voltage equation expressed in the stationary reference frame, as follows

$$\frac{d}{dt}\Phi s = V_s - r_s i_s \tag{14}$$

where, V_s stator voltage vector, i_s and r_s are the current vector and resistance respectively. Neglecting the voltage drop $r_s i_s$ across the stator resistance, and taking into account that the voltage vector is constant in each sampling period (T_s), stator flux vector variation turns is proportional to the applied voltage vector.

For Constant value of stator flux, the changing of the electromagnetic torque T_{em} based on the applied voltage vector's directions, such that:

$$T_{em} = N_p \frac{M}{l_r l_s - M^2} \|\Phi_s\| \|\Phi_r^s\| \sin\delta \tag{15}$$

where, Φ_r^s, named as rotor flux is referred to the stator, δ is the angular shift between the stator and rotor flux, N_p is the number of polesand l_s, l_r are the stator self-inductance and the rotor self-inductance respectively. The mutual inductance denoted by M.

2.3 DTC Scheme for Two Level VSI Topology

Stator flux is derived from equation[7] is given by

$$\hat{\lambda}_s^a = \int (\hat{v}_s^a - \hat{i}_s^a R_s) dt \tag{16}$$

where, $\hat{v}_s^a$ and $\hat{i}_s^a$ are the measured the voltage and current respectively. The classical control of DTC with two level inverter is shown in Figure 1. Electromagnetic torque is derived from equation[13] is given by

$$\hat{T}_e = \frac{3P}{4}(\hat{\lambda}_{ds}^a \hat{i}_{qs}^a - \hat{\lambda}_{qs}^a \hat{i}_{ds}^a) \tag{17}$$

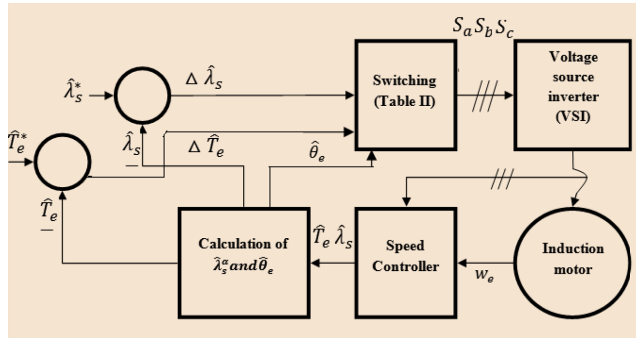

Figure 1. Classical DTC scheme with two-level inverter.

The operating status of the switches in the two-level inverter shown in Figure 2 can be represented by switching states. Switching states are defined by torque error and flux errors shown in Table 1 and Table 2.

Reference voltage is derived from α and β reference frame below[18].

$$\vec{V}_{ref} = V_\alpha + jV_\beta = \frac{2}{3}(V_a + aV_b + a^2 V_c) \tag{18}$$

Similarly,

$$|\vec{V}_{ref}| = \sqrt{V_\alpha^2 + V_\beta^2}, \quad \alpha = tan^{-1}\left(\frac{v_\beta}{v_\alpha}\right)$$

$$v_\alpha = jV_\beta = \frac{2}{3}\left(V_a + e^{j\frac{2\pi}{3}} V_b + e^{-j\frac{2\pi}{3}} V_c\right) \tag{19}$$

$$v_\alpha = jV_\beta = \frac{2}{3}\left(V_a + cos\frac{2\pi}{3}V_b + V_a + cos\frac{2\pi}{3}V_c\right) + j\frac{2}{3}\left(sin\frac{2\pi}{3}V_b - sin\frac{2}{3}V_c\right) \tag{20}$$

By equating the real and imaginary parts derived by,

$$V_\alpha = \frac{2}{3}\left(V_a + cos\frac{2\pi}{3}V_b + cos\frac{2\pi}{3}V_c\right)$$

$$V_\beta = \frac{2}{3}\left(0V_a + sin\frac{2\pi}{3}V_b - sin\frac{2\pi}{3}V_c\right)$$

$$\begin{bmatrix} V_d \\ V_q \end{bmatrix} = \frac{2}{3}\begin{bmatrix} 1 & cos\frac{2\pi}{3} & cos\frac{2\pi}{3} \\ 0 & sin\frac{2\pi}{3} & sin\frac{2\pi}{3} \end{bmatrix} \cdot \begin{bmatrix} V_a \\ V_b \\ V_c \end{bmatrix} \tag{21}$$

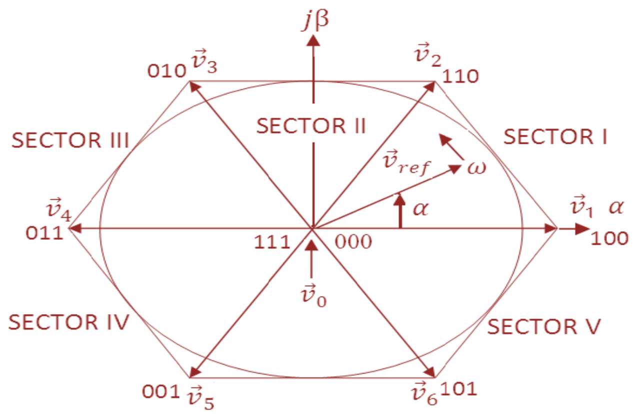

Figure 2. Space vector diagram for two level inverter.

Table 1. Switching State of VSI

State	Leg A			Leg B			Leg C		
	S_1	S_4	V_{an}	S_3	S_6	V_{bn}	S_5	S_2	V_{cn}
1	on	off	V_d	on	off	V_d	on	off	V_d
0	off	on	0	off	on	0	off	on	0

Table 2. Switching State of Space Vector

Space vector		Switching state (three phases)	ON-state switch	Definition
Zero vector	$\vec{V}_1$	[1 1 1]	S_1, S_3, S_5	0
		[0 0 0]	S_4, S_6, S_2	
Active vector	$\vec{V}_2$	[1 0 0]	S_1, S_6, S_2	$\vec{V}_1 = \frac{2}{3}V_d e^{j0}$
	$\vec{V}_3$	[1 1 0]	S_1, S_3, S_2	$\vec{V}_1 = \frac{2}{3}V_d e^{j\frac{\pi}{3}}$
	$\vec{V}_4$	[0 1 0]	S_4, S_3, S_2	$\vec{V}_1 = \frac{2}{3}V_d e^{j\frac{2\pi}{3}}$
	$\vec{V}_5$	[0 1 1]	S_4, S_3, S_5	$\vec{V}_1 = \frac{2}{3}V_d e^{j\frac{3\pi}{3}}$
	$\vec{V}_6$	[0 0 1]	S_4, S_6, S_5	$\vec{V}_1 = \frac{2}{3}V_d e^{j\frac{4\pi}{3}}$
	$\vec{V}_7$	[1 0 1]	S_1, S_6, S_5	$\vec{V}_1 = \frac{2}{3}V_d e^{j\frac{5\pi}{3}}$

3. DTC Scheme for Three level NPC Topology

Switching states that are shown in Figure 3 can constitute the operating status of the switches in the three-level inverter. When switching state is '1', it is specified that upper two switches in leg A connected and the inverter terminal voltage V_{AZ}, which means the voltage for terminal A with respect to the neutral point Z, is +E, whereas '–1' denotes that the lower two switches are ON, which means V_{AZ} = –E. When switching state '0', it indicates that the inner two switches S_2 and S_3 are connected and V_{AZ} = 0 through the clamping diode and load current directions. Switching status for leg A. Leg B and leg C shown in Table 3.

4. A Simple SVM (Space Vector Modulation Scheme)

The three-level Voltage Vector diagram is shown in Figure 4. There are six sectors (S_1-S_6), four triangles (Δ_0-Δ_3) in a sector, and a total of 27 switching states in this space vector diagram shown in Figure 5. As a method outlined in[22] advices, proposed space vector topology in each sector is segregated by four triangles, indexed as shown in Figure 6 every triangle examine as a single sector in two level hexagon scheme with the same sacking at the origin.

In this method, the triangle that hurdle the reference vector is indentified based on correlates thetip of the ref-

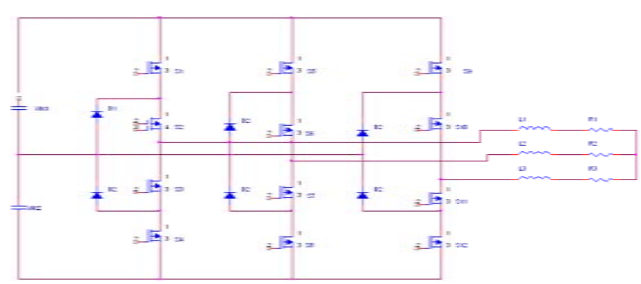

Figure3. Proposed NPC inverter circuit.

Table 3. Switching State of NPC

Switching State	Device switching status (phase A)				Inverter terminal voltage V_{AZ}
	S_1	S_2	S_3	S_4	
1	on	on	off	off	E
0	off	On	on	Off	0
–1	on	off	on	on	-E

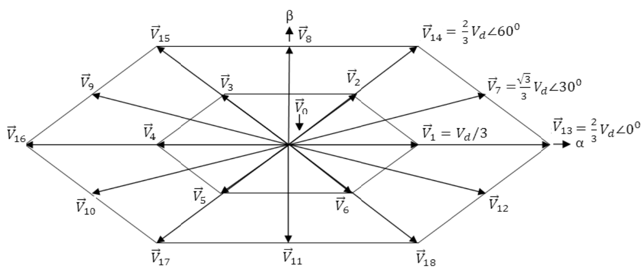

Figure 4. Space vector diagram of three-level inverter.

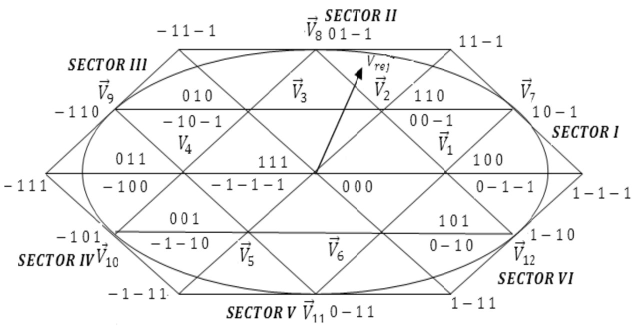

Figure 5. Sector division and Regions for three-level NPC.

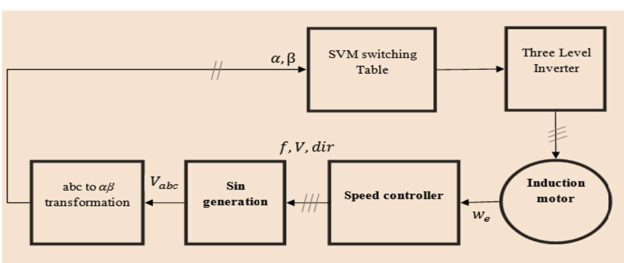

Figure 6. Schematic Diagram for Proposed Control Strategy.

erence vector. The triangles are obtained by calculating auxiliary parameters k_1 and k_2 which are defined as:

$$K_1 = \left[V_\alpha + \frac{V_\beta}{\sqrt{3}} \right] \tag{22}$$

$$K_2 = \left[\frac{\frac{V_\beta}{\sqrt{3}}}{2} \right] \tag{23}$$

where, V_α and V_β are correlates the tip of the space vector, k_1 founds whether the small triangle is in the right-hand side ($k_1 = 1$) or in the left-hand side ($k_1 = 0$). k_2 Founds if it is in the upper half ($k_2 = 1$) or in the lower half ($k_2 = 0$).

While reference vector is shifted to the new set of axes that intersect at the main crestof the triangle. In single triangle, the coordinates of the tip of the shifted reference vector $\overline{A_i P}$, where $P = V_\alpha$, V_β is the tipoff the original space vector and A_i is the origin of the triangle, are found as follows,

$$V_{\alpha i} = V_\alpha - K_1 + \frac{1}{2} k_2 \tag{24}$$

$$V_{\beta i} = V_\beta - \frac{\sqrt{3}}{2} k_2 \tag{25}$$

The triangle index is obtained by $\Delta = k_1^2 + 2k_2$

t_a (duration of the space-vector aligned with the α-axis), t_b (duration of the space-vector at 60° from the α-axis) and t_Z (duration of zero space-vectors) can be obtained by shifted coordinates follows.

$$t_a = t_s \left(V_{\alpha i} - \frac{V_{\beta i}}{\sqrt{3}} \right) \tag{26}$$

$$t_b = t_s \left(\frac{\frac{V_{\beta i}}{\sqrt{3}}}{2} \right) \tag{27}$$

$$t_z = t_s - t_a - t_b \tag{28}$$

The three neighboring space vectors are used to integrate the reference vector. These vectors resembled with vertices of the bounding triangle. The vector sequence in the first sector is determined through analysis. In other sectors, the states are obtained from the mapping of switching states between the first sector and other sectors. The switch states are remains constant for the first sector, but other sectors are negligible accordingly so that they use the available space-vector in other sectors.

In this paper the DTC-SVM scheme applied instead of hysteresis band, regulate the torque and the magnitude of flux is utilized by means of three-level inverter. Figure 7 shows the block diagram of the DTC-SVM with PI regulators

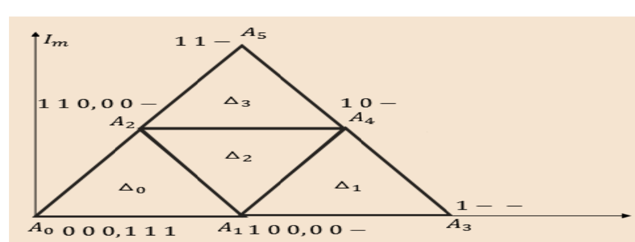

Figure 7. Sector Division to Four Triangles.

and three- level inverter. proposed method control both the torque and the magnitude of flux, thereby generating the voltage command for inverter control. mainly no decoupling mechanism is required as the flux magnitude and the torque can be regulated by the PI controllers. DTC based two-level and DTC-SVM three level schemes are implemented in simulation shown in section-5.

5. Simulation Results

DTC scheme are introduced which is Improve the induction motor performances via torque ripple reduction. Phase voltage and current waveform for two-level shown in Figure 8 (a,b). Torque and flux ripple performance and with speed and current waveform shown in Figure 8 (c,d,e).The Proposed DTC-SVM for NPC inverter fed induction motor simulation results are which is current and voltage waveform shown in Figure 9 (a,b).The Torque Ripple and flux performance with stator current and speed for three-level NPC inverter scheme shown in Figure 9 (c,d,e). The comparison performance shows that proposed scheme has an adequate solution to minimizing the torque with high speed operations.

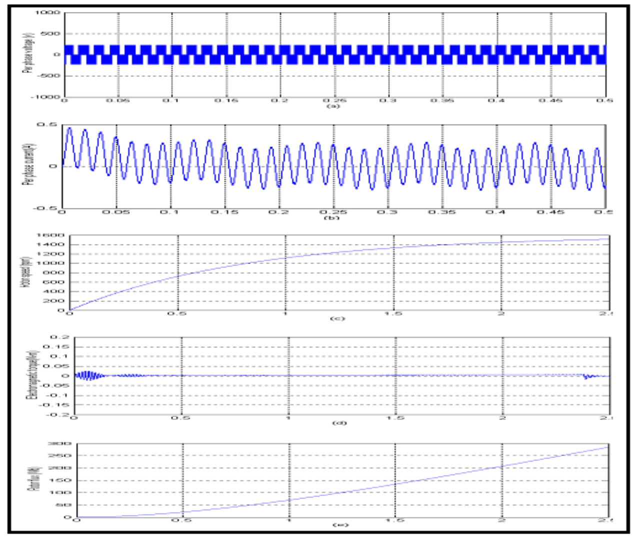

Figure 9. Neutral point clamped inverter performance: (a) per phase voltage (v) (b) Stator current (A) (c) Rotor speed (rpm) (d)Electromagnetic torque (N-m) and (e) Flux (Wb).

6. Conclusions

This paper deal with comparison and study about two level inverter DTC scheme and a simple space vector based three-level NPC inverter fed Induction motor for Torque Control. Proposed three level neutral point clamped inverter obtained the better torque and flux response through a simple space vector scheme. A simple space vector is generated using torque reference generation. NPC inverter scheme is improved the torque response by controlling the phase current over two level inverter scheme and easy control of DC-Link capacitor voltage balancing and torque control loop. Simulation results are obtained in both topologies. A simple space vector Three-level NPC inverter scheme obtained better torque control over Two-level inverter scheme using single control loop.

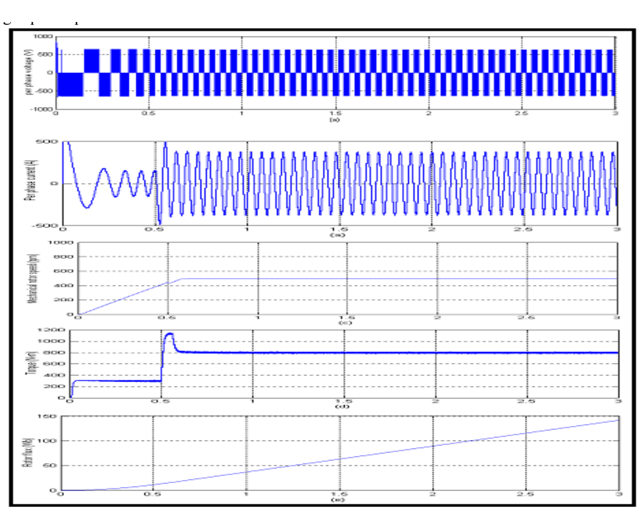

Figure 8. Two level inverter performance: (a) per phase voltage (v) (b) Stator current (A) (c) Rotor speed (rpm) (d) Electromagnetic torque (N-m) and (e) Flux (Wb).

7. Appendix

The parameters of Induction Motor
$0.5hp$, $50Hz$, $1500rpm$, $p = 4$ $R_s = 24, 6\Omega$, $R_r = 17.9\Omega$ $L_s = 984mH$, $L_r = 98.4mH$, $L_m = 914mh$ $J = 2.5kg.m^2$, $\beta = N.m.s$

8. References

1. Konstantopoulos GC, Alexandridis AT, Mitronikas ED. Bounded nonlinear stabilizing speed regulators for VSI-Fed induction motors in field-oriented operation. IEEE Transactions on Control Systems Technology. 2014 May; 22(3):1112–21.

2. Lee KB, Song JH, Choy I, Yoo JY. Torques ripples reduction in DTC of induction motor driven by three-level inverter with low switching frequency. IEEE Transactions on Power Electronics. 2002 Mar; 17(2):255–64.
3. Ambrosia V, Buja GS, Menis R. Band-constrained technique for direct torque control of induction motor. IEEE Transactions on Industrial Electronics. 2004 Aug; 51(4):776–84.
4. Maheshwari R, Munk-Nielsen S, Busquets-Monge S. Design of neutral-point voltage controller of a three-level NPC inverter with small DC-link capacitors. IEEE Transactions on Industrial Electronics. 2013 May; 60(5):1861–71.
5. Gholinezhad J, Noroozian R. Analysis of cascaded H-bridge multilevel inverter in DTC-SVM induction motor drive for FCEV. Journal of Electrical Engineering & Technology. 2013 Mar; 8(2):304–15.
6. Beerten J, Verveckken J, Driesen J. Predictive direct torque control for flux and torque ripple reduction. IEEE Transactions on Industrial Electronics. 2010 Jan; 57(1):404–12.
7. Basu K, Prasad JS, Narayanan G, Krishnamurthy HK, Ayyanar R. Reduction of torque ripple in induction motor drives using an advanced hybrid PWM technique. IEEE Transactions on Industrial Electronics. 2010 Jun; 57(6):2085–91.
8. Ramesh V, Latha YK. PFC-based control strategies for four switch VSI fed BLDC motor. Indian Journal of Science and Technology. 2015 Jul 7;8(16):1–6.DOI: 10.17485/ijst/2015/v8i16/70427
9. Lee KB, Song JH, Choy I, Choi JY, Yoon JH, Lee SH. Torque ripple reduction in DTC of induction motor driven by 3-level inverter with low switching frequency. Power Electronics Specialists Conference, 2000. PESC 00. 2000 IEEE 31st Annual; 2000. p. 448–53.
10. Lee KB, Song JH, Choy I, Yoo JY. Torque ripples reduction in DTC of induction motor driven by three-level inverter with low switching frequency. IEEE Transactions on Power Electronics. 2002 Mar; 17(2):255–64.
11. Takahashi I, Ohmori Y. High-performance direct torque control of an induction motor. IEEE Transactions on Industry Applications. 1989 Mar; 25(2):257–64.
12. Depenbrock M. Direct Self-Control (DSC) of inverter-fed induction machine. IEEE Transactions on Power Electronics. 1988 Oct; 3(4):420–9.
13. Boulghasoul Z, El Bahir L, Elbacha A, Elwarraki E. Adaptive-Predictive Controller based on Continuous-Time Poisson-Laguerre Models for Induction Motor Speed Control Improvement. Journal of Electrical Engineering & Technology. 2014 May 1; 9(3):908–25.
14. Zhang Z, Thomsen OC, Andersen M. Discontinuous PWM modulation strategy with circuit-level decoupling concept of three-level Neutral-Point-Clamped (NPC) inverter. IEEE Transactions on Industrial Electronics. 2013 May; 60(5):1897–906.
15. Dordevic O, Jones M, Levi E. A comparison of carrier-based and space vector PWM techniques for three-level five-phase voltage source inverters. IEEE Transactions on Industrial Informatics. 2013 May; 9(2):609–19.
16. Song W, Feng X, Smedley KM. A carrier-based PWM strategy with the offset voltage injection for single-phase three-level neutral-point-clamped converters. IEEE Transactions on Power Electronics. 2013 Mar; 28(3):1083–95.
17. Zaimeddine R, Berkouk EM, Refoufi L. A Scheme of EDTC control using an induction motor three-level voltage source inverter for electric vehicles. Journal of Electrical Engineering & Technology. 2007 Dec; 2(4):505–12.
18. Lai YS, Chen JH. A new approach to direct torque control of induction motor drives for constant inverter switching frequency and torque ripple reduction. IEEE Transactions on Energy Conversion. 2001 Sep; 16(3):220–7.
19. Sankar AB, Seyezhai R. Development of active neutral point clamped multilevel inverter fed BLDC drive employing FPGA. Indian Journal of Science and Technology. 2015 Feb 1; 8(4):392–9.
20. Lai YS. Modeling and vector control of induction machines-A new unified approach. Power Engineering Society 1999 Winter Meeting, IEEE; 1999. p. 47–52.
21. Ismail MM. Improving the performance of the DTC saturated model of the induction motor in case of two level and three level VSI using GA and PSO algorithms. Electronics, Communications and Computers (JEC-ECC), 2012 Japan-Egypt Conference on IEEE; 2012 Mar. p. 79–84.
22. Kaura V, Blasko V. A new method to extend linearity of a sinusoidal PWM in the over modulation region. IEEE Transactions on Industry Applications. 1996 Sep; 32(5):1115–21.
23. Zhou K, Wang D. Relationship between space-vector modulation and three-phase carrier-based PWM: a comprehensive analysis [three-phase inverters]. IEEE Transactions on Industrial Electronics. 2002 Feb; 49(1):186–96.
24. Subhashini M, Latha P, Bhagyaveni MA. Comparative analysis of harmonic distortion of a solar PV fed cascaded H-bridge multilevel inverter controlled by FPGA and diode clamped inverter. Indian Journal of Science and Technology. 2015 Jul 7; 8(16):1–8.
25. Babu AR. Comparative analysis of cascaded multilevel inverter for phase disposition and phase shift carrier PWM for different load. Indian Journal of Science and Technology. 2015 Apr 1; 8(S7):251–62.